Finite element modeling and anisotropy implementation in 3D printed structures using an optimized method

Marouene Zouaoui[a,b*], Carl Labergere[a], Julien Gardan[a,b], Ali Makke[b], Naman Recho[b,c], Pascal Lafon[a]

a.Institut Charles Delaunay, LASMIS, UTT,UMR CNRS 6281, 12 rue Marie Curie, 10010 Troyes, France
b.EPF, Engineering school, 2 rue Fernand Sastre, Troyes, France
c.Pascal Institute, Blaise Pascal University, 63000 Clermont Ferrand, France

* Corresponding author. Tel.: +33 (0)3 25 71 76 00. E-mail address: marouene.zouaoui@utt.fr

Abstract

This work studies with the mechanical behavior of an adaptive material produced by Fused deposition modeling that had better respond to real loading state.Authors focus on the implementation, using finite element modeling, of 3D printed structures by Fused Deposition Modeling of the behavior Acrylonitrile Butadiene Styrene material obtained by an optimized deposition strategy. We extend a previous study [1], [2] that proposes a method of improving the fracture toughness by reproducing the principal stress directions during the generation of trajectories in the case of Compact Tension specimen . A recent work [3] proves the efficiency of this optimized deposition on the stress intensity factor values for notched bending specimen. The objective of this new study is to propose a model for the material's behavior taking into account the trajectories of filaments. The proposed method involves the local elements of the mesh to capture the trajectories of the filaments and associate them with references of Acrylonitrile Butadiene Styrene (ABS) material in ABAQUS.

Key words: Fused deposition modeling, Finite elements method, optimized deposition, reference's orientation, Fracture behavior

Nomenclature

|	
ABS	Acrylonitrile Butadiene Styrene
BEAM	Notched beam for bending test
CT	Compact Tension specimen
FDM	Fused Deposition Modeling
FEM	Finite Element Method
SIF	Stress Intensity Factor
3D	Three dimensional
FE	Finite element

1 Introduction

3D printing can be defined as turning a digital model into a physical three-dimensional object by adding material a layer at a time. This is where the alternative term additive manufacturing comes from. It is therefore a fundamentally different way of producing parts compared to traditional subtractive or forming manufacturing technologies. There are several different methods of 3D printing which deals with many types of materials [4]. However, these technologies suffer from anisotropic mechanical properties, which are introduced during the manufacturing process. This anisotropy affects directly the performance of the printed part. The anisotropy of FDM parts was studied by Ahn et al. [5]. The development of a numerical model to predict the mechanical behavior of 3D printed parts is then a mandatory step to optimize the use of such technologies. This proposed study is a part of an advanced structured materials area that aims to enhance mechanical properties. A combined computational and experimental study has been carried out to investigate the fracture of additively manufactured polymers as well as possible toughening mechanisms [6]. We consider a former research based on the deposition of filaments according to the principal stress directions [1]. The specific mechanical constraints from product's use are therefore respected while the generation of the trajectories. Improvement of the fracture toughness of CT specimen were highlighted. This work aims at intoducing filaments orientation in a numerical model to study fracture behavior of both CT and BEAM specimen [7]. Fracture modes [8] will be studied through the determination of the J integral and the stress intensity factor.

2 Materials and method

2.1 Deposition Criterion

The key idea starts by finding the principal stress directions under the loading conditions. For that, a 2D numerical simulation of the specimen using an isotropic behavior was used to provide the principal directions, which are computed at each point in the sample. The printing trajectory must be tangent to these directions so that a strengthening is guaranteed. The assumption of plane stress condition is made; therefore, there are two principal directions in the sample. Consequently, two trajectories are to be taken into account in the printing. For this reason, the thickness dimension of the sample is built by alternate layers. In order to simplify the slicing procedure, layers representing the same principal direction are gathered in groups. Instead of changing the deposition orientation every layer, each group of layers are printed respecting the same principal direction. Only the region where fracture is more likely to occur is going to be printed using the optimization method. In order to do that, modification of the G-code are to be made. The Figure 1 shows the strategy applied on the CT specimen before the execution of the mechanical test.
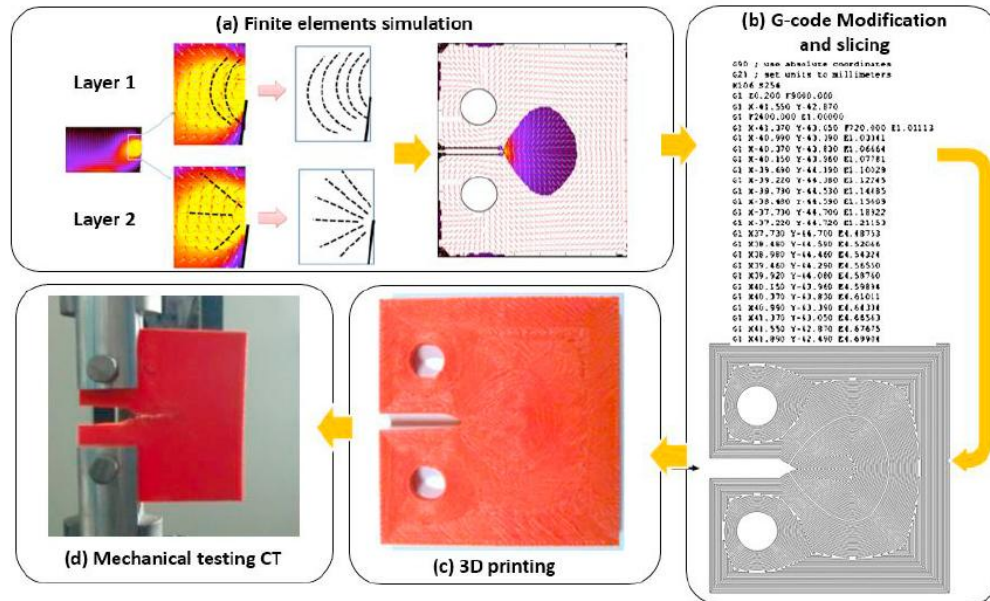
Fig. 1. *Optimization of the deposition method used on the CT specimen before the mechanical test stage[1]*

2.2 CT and BEAM specimen

Two types of specimen are to be studied (classical ones printed using +45°/-45° orientations and optimized) in order to highlight the effect of the optimized deposition method. Both specimen present a mode I fracture so results found for the CT specimen are going to be used for the BEAM ones. The geometries used are those described in [7] and [9] for mode I fracture. A Makerbot replicator x2 3D printer was used to print the specimen. First layer had a different thikcness to ensure a good printing quality. ABS layers were printed at a temperature of 235°C. The open source 3D printing toolbox Slic3r is then used to generate a first version of the G-Code that will be post processed, as it will be described in the next section. To prepare the owner/proprietor file to be inserted into the 3D printer, Replicator G was used.

2.3 Material behavior

Tensile specimen ASTM 638 I were printed with the same set of printing parameters while changing raster orientation. Two orientations were tested: 0° and 90°. An orthotropic behavior is proposed by the authors to study the behavior of ABS. If we consider the longitudinal direction of the filaments as direction number 1, we can assume that the transverse direction 2 and 3 will have the same behavior thanks to the similarity of the structure (see Figure 2). The only difference is the welding surface, which is larger for filaments deposed in the direction 2.
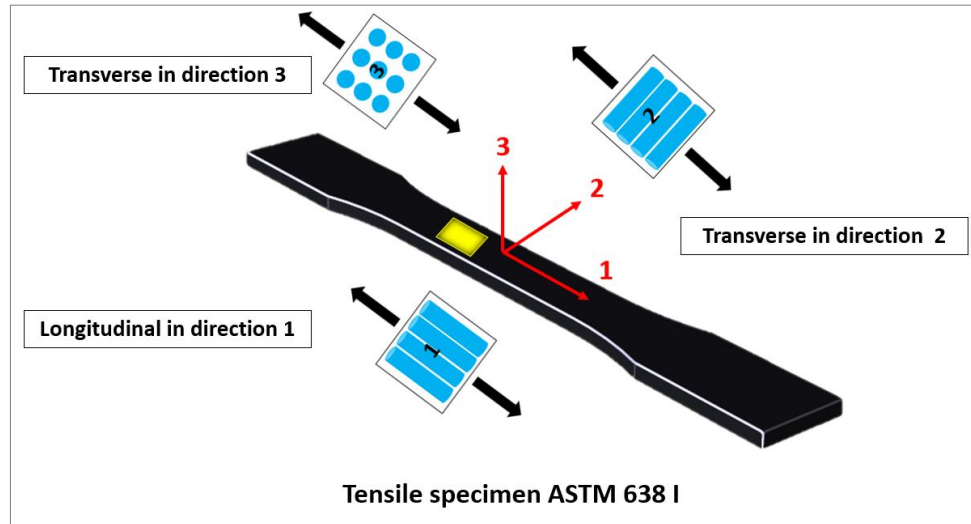
Fig. 2. *Filaments orientation for the tensile tests*

For orthotropic behavior, a model implemented in ABAQUS is used where the stress is expressed according to the stiffness matrix and the strain field. Such model needs the values of the Young's modulus and Poisson's ratio in transverse and longitudinal directions and then shear modulus in the XY plane and XZ plane and YZ plane. Shear modulus was calculated via the classical expression using Young's modulus and Poisson's ratio values. Moreover, it was supposed to be the same for all shear planes. The average values of the Young's modulus calculated basing on the tensile curves are presented in the following table.

Tab. 1. *Summary of the tensile tests*

Raster orientation	Young's modulus (MPa)	Poisson's ratio	Average Shear modulus (MPa)
0° (direction 1)	1484.3	0.33	$G = \frac{E}{2(1+\upsilon)} = 503.9$
90° (direction 2)	1176.7	0.31	

In order the use the orthotropic behavior using ABAQUS, the components of the stiffness matrix (see Equation 1) must be given as inputs.

$$\begin{pmatrix} \sigma_{11} \\ \sigma_{22} \\ \sigma_{33} \\ \sigma_{12} \\ \sigma_{13} \\ \sigma_{23} \end{pmatrix} = \begin{bmatrix} D_{1111} & D_{1122} & D_{1133} & & & \\ D_{1122} & D_{2222} & D_{2233} & & 0 & \\ D_{1133} & D_{2233} & D_{3333} & & & \\ & & & D_{1212} & & \\ & 0 & & & D_{1313} & \\ & & & & & D_{2323} \end{bmatrix} \begin{pmatrix} \varepsilon_{11} \\ \varepsilon_{22} \\ \varepsilon_{33} \\ \gamma_{12} \\ \gamma_{13} \\ \gamma_{23} \end{pmatrix} \qquad \textbf{\textit{Eq. 1}}$$

Where:

$$D_{1111} = E_1(1 - \nu_{23}\nu_{32})\gamma \qquad \textbf{\textit{Eq. 2}}$$

$$D_{2222} = E_2(1 - \nu_{13}\nu_{31})\gamma \qquad \textbf{\textit{Eq. 3}}$$

$$D_{3333} = E_3(1 - \nu_{12}\nu_{21})\gamma \qquad\qquad \textbf{\textit{Eq. 4}}$$

$$D_{1122} = E_1(\nu_{21} + \nu_{31}\nu_{23})\gamma = E_2(\nu_{12} + \nu_{32}\nu_{13})\gamma \qquad\qquad \textbf{\textit{Eq. 5}}$$

$$D_{1133} = E_1(\nu_{31} + \nu_{21}\nu_{32})\gamma = E_3(\nu_{13} + \nu_{12}\nu_{23})\gamma \qquad\qquad \textbf{\textit{Eq. 6}}$$

$$D_{2233} = E_2(\nu_{32} + \nu_{12}\nu_{31})\gamma = E_3(\nu_{23} + \nu_{21}\nu_{13})\gamma \qquad\qquad \textbf{\textit{Eq. 7}}$$

$$D_{1212} = G_{12} \qquad\qquad \textbf{\textit{Eq. 8}}$$

$$D_{1313} = G_{13} \qquad\qquad \textbf{\textit{Eq. 9}}$$

$$D_{2323} = G_{23} \qquad\qquad \textbf{\textit{Eq. 10}}$$

$$\gamma = \frac{1}{1 - \nu_{12}\nu_{21} - \nu_{23}\nu_{32} - \nu_{31}\nu_{13} - 2\nu_{21}\nu_{32}\nu_{13}} \qquad\qquad \textbf{\textit{Eq. 11}}$$

The assumption of the unicity of the Poisson's ratio was made and an average value was calculated from the values found through the tensile tests. All the numerical values were computed into ABAQUS. For the use of such model, defining references is mandatory to fit the orthotropic direction. Knowing that filaments have different orientations because of the optimized deposition, local references should be defined at the level of elements to reproduce the same orientations.

2.4 Numerical modeling

Finite element code ABAQUS was used to simulate mechanical tests. The figure 3 shows the meshed specimens with respect to the slicing strategy. The maximum value of displacement corresponding to the limit of the elastic part of the curve of load versus displacements was identified. The given displacement value was applied on the mobile pin.
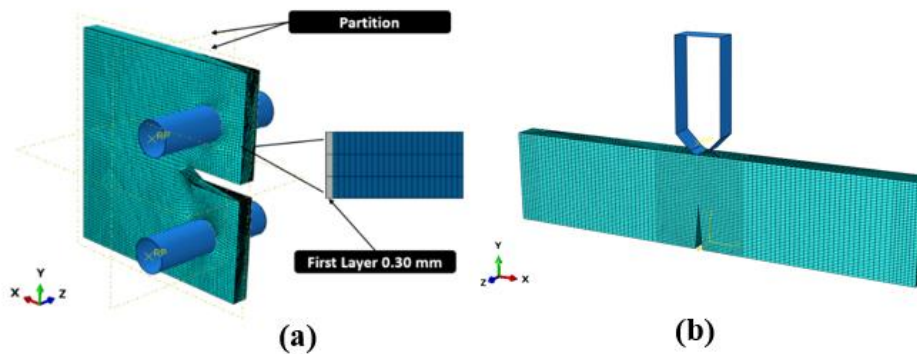
***Fig. 3.*** *Abaqus models of both specimen, (a): CT specimen and (b): BEAM specimen*

2.5 Assignment of the material's references orientation

The authors manage to export the trajectories of ABS deposition by analyzing the G-Code. Layers are identified through the Z coordinate thanks to a suitable mesh. Assigning material's references starts by capturing the trajectories, then associating them with the elements of the numerical model. The mesh being already generated, the file containing the coordinates of all

the nodes and indicating the number of elements was exported. For that, it was necessary to be able to know which trajectory passes by a certain element. It is already faster to focus on the layer to which our element belongs. Having inserted this assignment to a layer now allows limiting the search domain of the trajectories. To detect if a path belongs to an element, the intersections of the element with the faces of our element must be found. It is also possible to have trajectories included in an element so that there will be no intersection. Those ones must be identified and taken into account because once those intersections are identified; the domain in the G-Code where the trajectories are likely to be included in our element can be delimited. Once all the intersections and all the trajectories passing by an element are found, the goal was to calculate the direction vector of each trajectory and to make an average of these directions in order to represent at best the general direction of deposition. Gauss points were considered while identifying each element.

Limiting the trajectory search to the corresponding layer of which the element belongs make the identification easier. The following configuration (see Figure 4) reduces the problem to one element:

• **Case 1:** several trajectories belong to the element. The one that passes closest to the G auss points must be found.

• **Case 2:** several trajectories belong to the element but the point closest to its Gauss point is that of the discontinuity between the two trajectories. Here the method will consist in selecting the first trajectory analyzed. The printing order is respected here.

• **Case 3:** no trajectory belongs to the element. This could have been a problem with the intersection method between face and trajectory but here, even if this trajectory does not belong to the element, if it is closest to its Gauss point then it will be considered.
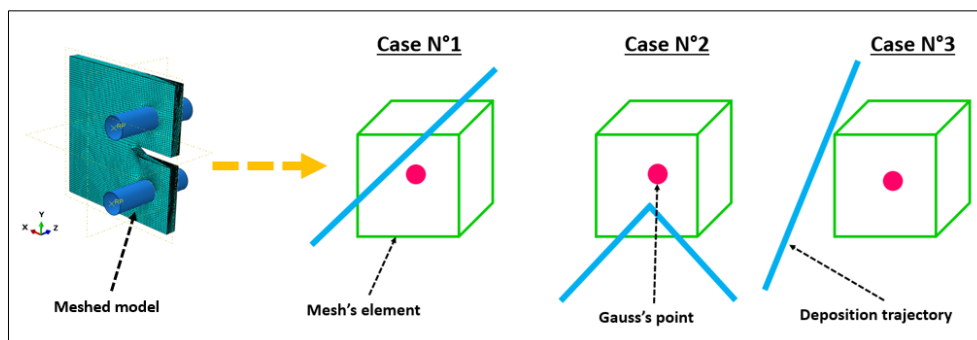
Fig. 4. *Assigning local references for mesh's elements*

The next figure shows the meshed CT specimen after assigning local references. Axe-1 (see figure 5) corresponds to the filament. An .inp file will be created and called while running the simulation in the main .inp file through the key word INCLUDE.
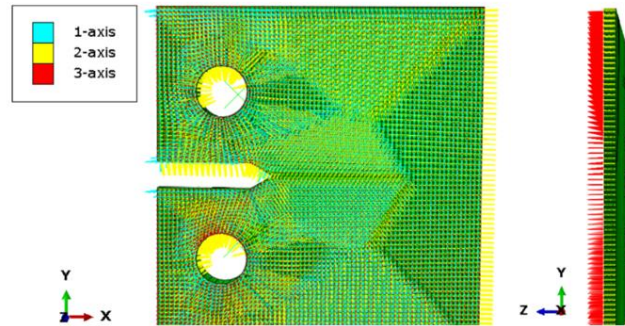
***Fig. 5.*** *Material's references assignment of one of the principal's directions for an optimized CT specimen*

3 Results and discussions

First results (see Figure 6 and 7) shows that orthotropy has almost no effect on the mechanical behavior in the elastic state and the assumption of isotropy can be made. References orientations will be used later to characterize the fracture behavior. Based on the tensile tests an average value for both Young's modulus and Poisson's ratio were used during the simulation. Values used in the numerical simulation are showed in the next table.

Tab. 2. *Elastic constant calibrated in the elastic state based on the mechanical tests*
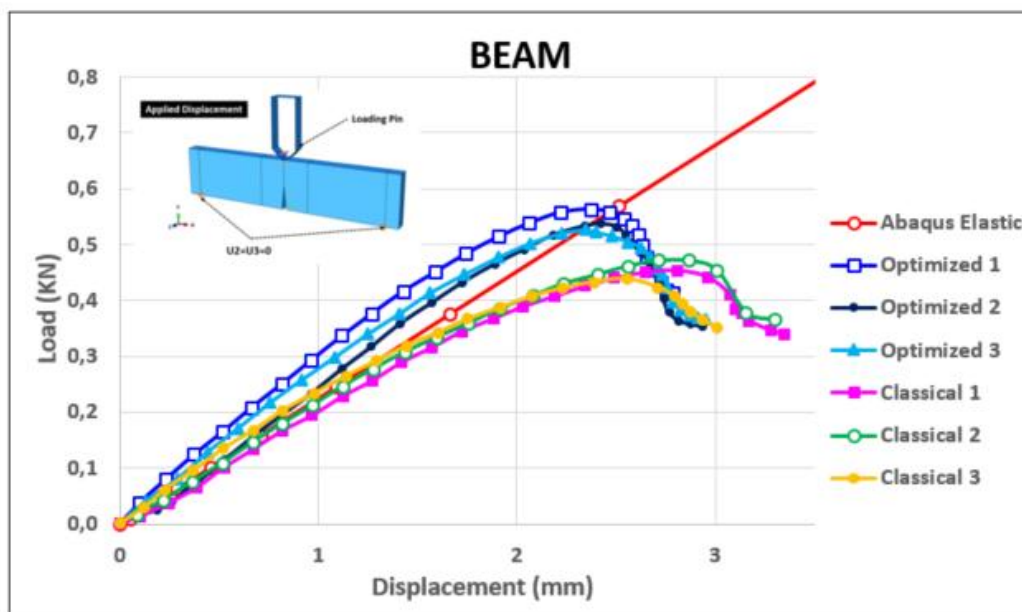
Young's modulus (MPa)	Poisson's ratio
1330.1	0.32

Simulations that used those values (see table) shows a good agreement with experimetal data. For the CT specimen an average experimental stiffness that represents the load level for an increment of displacement (N/mm) was found equal to 666 N/mm for the optimized specimen and 650 N/mm for the classical one [10]. However, numerical model has a greater value by 200 N/mm, which can possibly be related to the isotropy assumption. It was suggested that the heterogeneity induced by the weld lines and especially the air gap reduce considerably the strength of the material. At this stage, the behavior was calibrated in the elastic state. To check the validity of the results we decided to simulate the bending test of BEAM specimen.

Load versus displacement

Load (N) vs *Displacement (mm)*

- Optimized
- Classical
- Abaqus-Isotropic
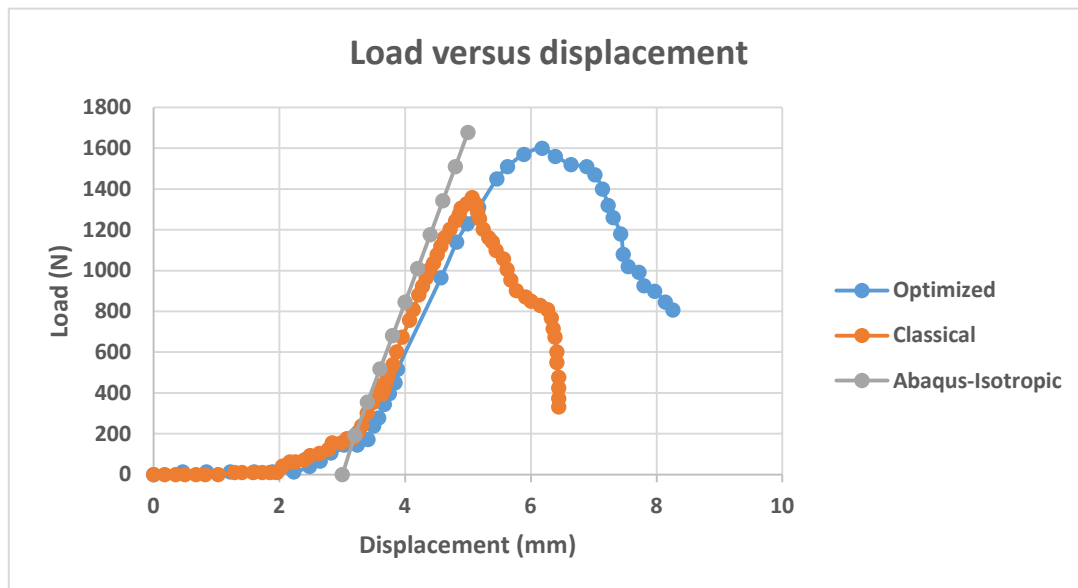
Fig. 6. *Average experimental results for the CT specimen [10]compared to the numerical simulation*

Figure 7 shows that the prediction of the numerical model is placed between both types of specimen for BEAM ones. Experimental data were collected from the work of Lanzillotti and al [3] that consider three classical BEAM specimen and three optimized ones .This result is directly related to the anisotropy introduced while printing the specimen, which is not represented in the model. Generally, the results seem to be coherent. However, the influence of the optimization method is not significant. The study of the stress intensity factor can highlight this part and give further explanation about the fracture behavior of the material.

BEAM

Load (KN) vs *Displacement (mm)*

- Abaqus Elastic
- Optimized 1
- Optimized 2
- Optimized 3
- Classical 1
- Classical 2
- Classical 3

Fig. 7. *Evolution of load versus displacement for the BEAM specimen [3] (3 classical specimen and 3 optimized) and the numerical model*

8

Mechanical behavior of CT specimen and BEAM specimen made by Acrylonitrile Butadiene Styrene (ABS) material and fabricated by Fused Deposition Modeling were studied through numerical simulation. The numerical model captures the filaments trajectories and associates them with the ABS material's reference on ABAQUS. Orthotropic law was used. Such mechanical behavior has almost the same stress state of an isotropic material. The First reason to which authors relate such similarity is the small difference between the Young's modulu. Both the weld line and the air gap were neglected while considering the isotropy assumption. Further work will focus on an accurate characterization of the material constants that can highlight the effect of anisotropy inside the material. The plasticity will also be studied even when it is considered as a local phenomenon for the deposited material.

4 Conclusion

This study gives preliminary analysis of the mechanical behavior of a smart material printed using an optimized deposition. In the elastic state, the behavior appears to be isotropic although materials constants were not precisely obtained. The interaction between the filaments is an important factor that defines directly the material's strength. Future work will establish an identification method aiming to find the material's constants via Digital image correlation to implement more precise values in the simulation.

References

[1] J. Gardan, A. Makke, and N. Recho, "A Method to Improve the Fracture Toughness Using 3D Printing by Extrusion Deposition," *Procedia Struct. Integr.*, vol. 2, pp. 144–151, 2016.

[2] J. Gardan, A. Makke, and N. Recho, "Improving the fracture toughness of 3D printed thermoplastic polymers by fused deposition modeling," *Int. J. Fract.*, vol. 210, no. 1–2, pp. 1–15, Mar. 2018.

[3] P. Lanzillotti, J. Gardan, A. Makke, and N. Recho, "Enhancement of fracture toughness under mixed mode loading of ABS specimens produced by 3D printing," *Rapid Prototyp. J.*, Mar. 2019.

[4] J. Gardan, "Smart materials in additive manufacturing: state of the art and trends," *Virtual Phys. Prototyp.*, vol. 14, no. 1, pp. 1–18, Jan. 2019.

[5] S. Ahn, M. Montero, D. Odell, S. Roundy, and P. K. Wright, "Anisotropic material properties of fused deposition modeling ABS," *Rapid Prototyp. J.*, vol. 8, no. 4, pp. 248–257, Oct. 2002.

[6] J. Li, S. Yang, D. Li, and V. Chalivendra, "Numerical and experimental studies of additively manufactured polymers for enhanced fracture properties," *Eng. Fract. Mech.*, Nov. 2018.

[7] T. Keiichiro and I. Hitoshi, "Elastic-plastic fracture toughness test under mixed mode I-II loading," *Eng. Fract. Mech.*, vol. 41, no. 4, pp. 529–540, Mar. 1992.

[8] J. Li, X.-B. Zhang, and N. Recho, "J–Mp based criteria for bifurcation assessment of a crack in elastic–plastic materials under mixed mode I–II loading," *Eng. Fract. Mech.*, vol. 71, no. 3, pp. 329–343, Feb. 2004.

[9] ASTM data sheet: Designation: E 1820-01 Standard Test Method For Measurement of Fracture Toughness.

[10] J. Gardan, A. Makke, and N. Recho, "Fracture Improvement by Reinforcing the Structure of Acrylonitrile Butadiene Styrene Parts Manufactured by Fused Deposition Modeling," *3D Print. Addit. Manuf.*, Jun. 2018.